

Zn^{2+} Specific Colorimetric Receptor Based on Coumarin

Kaushal Kumar Upadhyay* and Rakesh Kumar Mishra

Department of Chemistry, Faculty of Science, Banaras Hindu University, Varanasi-221005, India

Received March 1, 2010; E-mail: drkaushalbhu@yahoo.co.in

The receptor **1** having coumarin and thiazole as electron-deficient and -rich centers respectively acted as a colorimetric receptor selectively for Zn^{2+} as its chloride salt in DMSO/aq. DMSO (10:90 v/v) by exhibiting a remarkable bathochromic shifting of 120 nm in its 375 nm UV–visible absorption band. The interaction of receptor **1** with a number of metal ions ranging from s,p to d blocks as their chloride salts indicated the selectivity of the same toward Zn^{2+}. Transmission electron microscopy (TEM) along with spectroscopic studies indicated Zn^{2+} triggered aggregate formation of the receptor **1** as the key step toward sensing.

Design and synthesis of chemosensors with capability of selective and effective detection of analytes have been gaining momentum for the last few decades.[1–4] The qualitative and quantitative determinations of trace metals have been a challenging task for chemists in view of their crucial roles in the physiology and biochemistry of living systems. In mammals Zn^{2+} is the second most abundant heavy metal ion after iron[5] and is an essential component of many protein scaffolds like carbonic anhydrase, carboxy peptidase, superoxide dismutase, etc.[6] At the same time it also plays important roles in various biological processes such as signal transduction, gene expression, neurotransmission, etc.[7–9] Zinc deficiency causes unbalanced metabolism, which in turn can induce retarded growth in children, male, and female reproductive problems, low blood sugar, poor bone growth, brain disorders, high blood cholesterol, etc.[10,11] Another important additive effect of zinc in our body is illustrated by zinc-binding proteins, such as metallothionein, which functions in lead detoxification by sequestering lead within the enterocyte.[12–14] Generally the total concentration of Zn^{2+} in different cells ranges from nanomolar to millimolar.[15] Therefore, there is a great need to design and develop zinc specific chemosensors which are able to detect and monitor the same selectively.

The present study derives from our continuous endeavor over the last couple of years toward synthesis of some cost effective naked eye receptors involving least synthetic complexity.[16–21] The colorimetric receptors have a clear edge over others as they do not involve any pretreatment of sample or costly instrumentation. They exhibit color changes upon analyte binding due to perturbation of their intramolecular charge transfer (ICT) bands which are a common feature of the UV–vis spectra of molecules having simultaneous presence of electron-rich and -deficient pockets.[22]

The reported sensors for Zn^{2+} in the literature so far have significant drawbacks which include their sensitivity toward group II and transition-metal ions or lacking of effective response toward Zn^{2+} in the presence of competitive d^{10} metal ions due to their similar chemical properties.[23–25] Keeping all these points in mind we thought it worthwhile to synthesize a new Zn^{2+} colorimetric sensor which would overcome all these drawbacks. The selection of coumarin as part of receptor **1** is based on literature reports regarding its involvement in a number of receptors for cations[26,27] besides its multiple pharmacological applications.[28,29]

Experimental

Apparatus. ^{1}H NMR spectral studies were performed on JEOL AL 300 FTNMR as well as Bruker-400 Avance NMR Spectrometers using tetramethylsilane (TMS) as an internal reference standard. The UV–vis spectral studies were performed on a UV-1700 pharmaspec spectrophotometer with qurtz cuvette (path length: 1 cm) while mass spectrometric analysis was carried out on a MDS Sciex API 2000 LCMS spectrometer. The IR spectrum for the receptor **1** was recorded on a JASCO-FTIR spectrophotometer. Transmission electron microscopic (TEM) studies were performed using Philips: CM-12 and FEI: Technai 20G2 electron microscopes.

Materials. All reagents for synthesis were purchased from Sigma-Aldrich and were used without any further purification. The spectroscopic grade dimethylsulfoxide (DMSO) for UV–visible experiments was purchased from Spectrochem pvt. Ltd. Mumbai, India.

General Procedures for the Metal-Ion Binding Studies. All titration experiments were carried out at room temperature. For the UV–visible titrations a 5×10^{-5} M solution of the receptor **1** and solutions of chloride salt of metals were prepared in DMSO/DMSO–H_2O (90:10 v/v). The ^{1}H NMR titrations were carried out in DMSO-d_6 using TMS as an internal reference standard. For the ^{1}H NMR spectral titrations the 5×10^{-3} M solutions of the receptor **1** and the varying equivalents of the chloride salts of Zn^{2+} were separately prepared in DMSO-d_6. The structures were fully optimized in the gas phase at the density functional theory (DFT) level with the Gaussian 03 package using B3LYP/6-31G** basis set.

Synthesis of Receptor 1. 2,2′-Bis{(*E*)-2-[1-(2-oxo-2*H*-chromen-3-yl)ethylidene]hydrazino}-4,4′-bi-1,3-thiazole, i.e., receptor **1** was synthesized by mixing 3-acetylcoumarinthiosemicarbazone (compound **3**) and 1,4-dibromobutane-2,3-dione in 2:1 molar ratio in methanol with constant stirring and gentle heating at ca. 60 °C for 2 h. To the stirred solution of

Published on the web October 5, 2010; doi:10.1246/bcsj.20100054

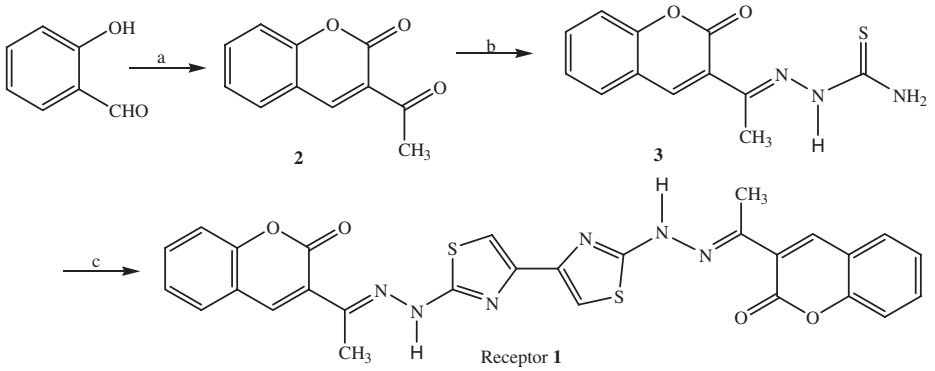

Scheme 1. Synthetic route of receptor **1**. Reagents and conditions: (a) Ethylacetoacetate, piperidine, EtOH, 0–5 °C; (b) thiosemicarbazide, EtOH, reflux 4 h; (c) 1,4-dibromobuta-2,3-dione, EtOH, stirring, 60 °C, 2 h.

3-acetylcoumarinthiosemicarbazone (0.261 g, 1.0 mmol) in 20 mL methanol, a solution of 1,4-dibromobutane-2,3-dione (0.121 g, 0.5 mmol) in 10 mL methanol was slowly added with constant stirring. The stirring along with mild heating ca. 60 °C was further continued for 2 h resulting into yellow solid which was filtered and dried over a pump. The above product was basified with aqueous $NaHCO_3$ leading to formation of free base i.e., receptor **1** followed by its recrystallization from DMSO–H_2O mixture (50:50, v/v). Receptor **1** was characterized through IR, ^1H and ^{13}C NMR spectral studies along with its mass determination through LC-MS and HRMS (see ESI, Figures S1–S4). IR ν/cm^{-1}: 3443, 2924, 1716, 1609, 1566, 1454, 1369, 1300, 1234, 1134, 1028, 964, 757, 633, 462; ^1H NMR (400 MHz, DMSO-d_6): δ 2.28 (s, 6H, CH_3), 7.04 (s, 2H, H-Ar), 7.37–7.45 (m, 4H, H-Ar), 7.63–7.67 (t, 2H, H-Ar), 7.84–7.86 (d, 2H, H-Ar), 8.17 (s, 2H, H-Ar), 11.47 (s, 2H, –NH); ^{13}C NMR (75 MHz, DMSO-d_6): δ 16.26, 105.17, 116.02, 118.95, 124.82, 126.57, 129.11, 132.28, 140.80, 145.30, 153.32, 159.21, 169.48; MS m/z (ESI) 569.00, Calcd for $C_{28}H_{20}N_6O_4S_2$: 568.10; HRMS ($C_{28}H_{20}N_6O_4S_2$) Theoretical 569.1066, Experimental 569.1065.

The synthesis of the receptor **1** may be presented conveniently through Scheme 1 as follows. Compounds **2** and **3** were synthesized according to reported methods.[30,31]

Results and Discussion

DFT Studies on Receptor 1. The quantum mechanical calculations at the DFT level using B3LYP/6-31G** basis set through Gaussian 03 package[32] were performed on receptor **1** in order to support its structural characterization through spectroscopic studies along with its mass determination as described above. The resulting energy minimized structure along with its HOMO–LUMO orbitals have been shown in Figures 1a and 1b. As can be seen, the receptor **1** is a symmetric molecule with two identical halves positioned in antagonistic way having one coumarin and one thiazole in each half. The highest occupied molecular orbital i.e., HOMO and lowest unoccupied molecular orbital i.e., LUMO of receptor **1** are localized mainly on the thiazole and coumarin moieties making them electron-rich and -deficient centers respectively. By virtue of incorporating the electron-rich and -deficient centers within the same molecule receptor **1** is a good example of a push–pull system and is a potential intramolecular charge transfer (ICT) probe of acceptor–donor–acceptor (A–D–A) type.

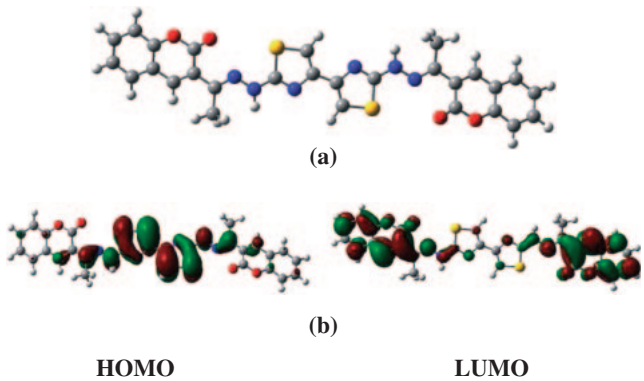

Figure 1. (a) Energy minimized structure of receptor **1** through DFT using B3LYP/6-31G** basis set. (b) DFT-computed HOMO, LUMO orbitals of receptor **1** with the correlation functional B3LYP and a 6-31G** basis set.

Zn^{2+} Binding Studies. The colorimetric recognition of Zn^{2+} by receptor **1** was studied through UV–vis spectrophotometric studies (Figure 2) involving concomitant additions of Zn^{2+} as its chloride salt to a 5×10^{-5} M DMSO solution of receptor **1**. Receptor **1** itself exhibited two absorption bands with their maxima at 278 and 375 nm due to π–π^* and n–π^* transitions respectively.[33]

On gradual additions of Zn^{2+} to the above receptor **1** solution, there was almost no effect on the visual and spectral characteristics of receptor **1** until the level of addition reached forty equivalents resulting in bathochromic shifting of 278 and 375 nm bands to 325 and 495 nm respectively. Simultaneously the visual appearance of the DMSO solution of receptor **1** at this stage changed from yellow to red. The new bands at 325 and 495 nm were assigned as metal-induced intramolecular charge transfer (MICT)[34] due to complexation of receptor **1** with Zn^{2+}. The visual and spectral changes in receptor **1** kept on intensifying further up to addition of 100 equivalents of Zn^{2+}. Further additions of the same did not affect the visual intensity but the spectral intensity of receptor **1** was affected to a minor extent. Finally a beautiful titration pattern as shown above in Figure 2 with three well-defined isosbestic points at 305, 350, and 423 nm indicating a neat interconversion

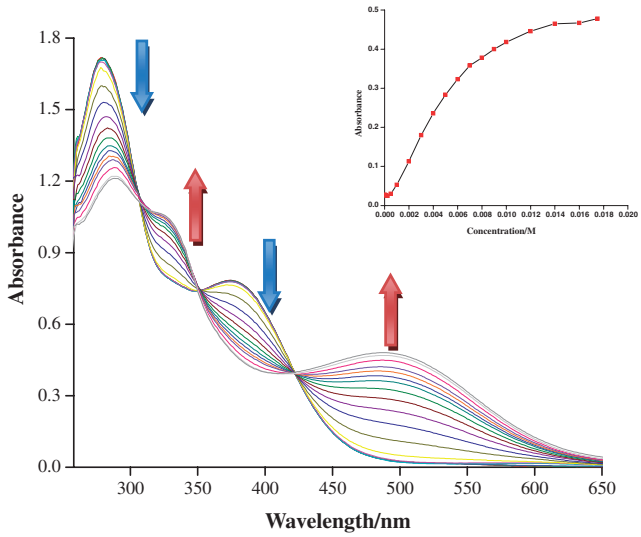

Figure 2. Showing titration pattern of receptor **1** in DMSO in the presence of varying amount of $ZnCl_2$ (0–300 equivalents). The plot of absorbance at 495 nm vs. concentration of $ZnCl_2$ added (inset).

Figure 3. Visual color changes of receptor **1** (1×10^{-4} M, DMSO) in the presence of 100 equivalents of different metal ions (from left to right) receptor **1**; **1** + Zn^{2+}; **1** + Cd^{2+}; **1** + Hg^{2+}; **1** + Mn^{2+}; **1** + Ni^{2+}; **1** + Cu^{2+}; **1** + Na^{+}; **1** + Ba^{2+}; **1** + Al^{3+}; **1** + Pb^{2+}.

between receptor **1** and its complex species with Zn^{2+} in the solution emerged during the course of titration.

The red shift of ca. 50 nm in the 278 nm band was attributed to the intramolecular complexation of Zn^{2+} by ketimine N and O atoms of receptor **1** hence creating electron defficiency at the coumarin center leading flow of electron density from thiazole to coumarin (ESI; Figure S12, stage A). However the massive red shift of 120 nm observed in the 375 nm band was attributed to Zn^{2+} driven deprotonation of receptor **1** triggering aggregate formation (ESI; Figure S12, stage B) which is most likely in the light of its DFT optimized structure. This deprotonation increases electron density on thiazole (HOMO) i.e., donor to a large extent leading to its pumping toward the acceptor i.e., the coumarin moiety (LUMO) resulting in the above-mentioned bathochromic shift. In order to establish the selectivity of receptor **1** toward Zn^{2+} the same was treated with a series of 100 equivalents of individual metal ions as their chloride salts.

As can be seen in Figure 3 Zn^{2+} is the only cation where a categorical naked eye change was observed however a poor naked eye change was also seen with Cu^{2+} but the corresponding spectral changes in the visible region were ill defined (ESI, Figure S5). On the other hand the spectral changes in the UV region were larger than Zn^{2+} but those were of no use from the viewpoint of naked eye change. The corresponding spectral

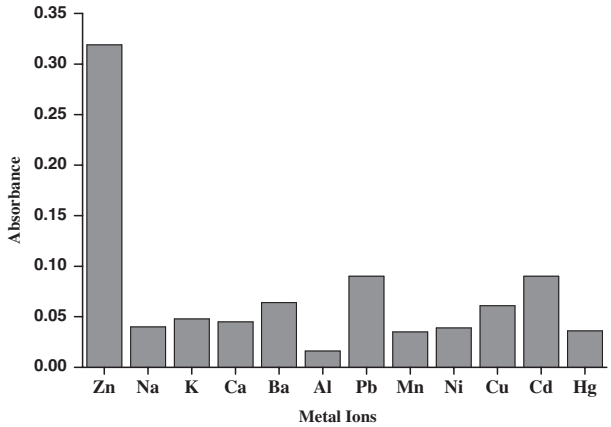

Figure 4. Bar graph representation of relative absorption intensity at 495 nm wavelength in the presence of 100 equivalents of M^{n+} (as their chloride salts).

changes in the UV–vis spectrum of receptor **1** on indivdual addition of respective ions have been given in ESI (Figure S6). The corresponding intensities of the 495 nm band for each metal ion have been shown in the form of bar graph in Figure 4. Neither naked eye (Figure 3) nor significant UV–vis spectral changes were produced in terms of shifting of 375 nm band to 495 nm band on addition of the heavier congeners of Zn^{2+}-like Cd^{2+} and Hg^{2+} establishing a clear superiority of Zn^{2+} in terms of its naked eye sensing. On the other hand few 3d congeners of Zn^{2+} viz. Mn^{2+}, Ni^{2+}, and Cu^{2+} were also able to produce spectral changes in the UV region of receptor **1** which were irrelevant from the view point of their naked eye sensing. Thus UV–vis titration studies of receptor **1** with a series of metal ions as their chloride salts established a fair superiority of Zn^{2+} over other meal ions in terms of naked eye sensing. The time dependent UV–vis spectral titration between receptor **1** and Zn^{2+} did not produce any meaningful information as there was no change in the spectral pattern of the same with respect to variation of time (ESI, Figure S7).

Competition experiments were also performed by adding a mixture of the above-mentioned metal ions along with Zn^{2+} as their chloride salts to the 5×10^{-5} M DMSO solution of receptor **1** (ESI, Figures S8 and S9). Similar visible change from pale yellow to red (as it was observed on addition of Zn^{2+} only) with slightly lower intensity was observed. The comparative UV–vis spectral changes in the 495 nm band was studied on the respective additions of 100 equivalents of a series of metal ions (Na^{+}, Ba^{2+}, Al^{3+}, Pb^{2+}, Mn^{2+}, Ni^{2+}, Cu^{2+}, Cd^{2+}, and Hg^{2+}) to a 5×10^{-5} M DMSO solution of receptor **1** with 100 equivalents of Zn^{2+}. Hence it is clear that although receptor **1** is binding with nearly all the chosen metal ions in the presence of Zn^{2+} but these bindings are not going to affect the selectivity of receptor **1** toward Zn^{2+} in terms of its colorimetric response.

Titrimetric studies between receptor **1** and Zn^{2+} as its chloride salt were also performed in aqueous DMSO (10:90 v/v) which resulted in similar visual and UV–vis spectral changes (ESI, Figure S10) with lower saturation limit at 100 equivalents of Zn^{2+} as compared to 300 equivalents of the same in dry DMSO possibly due to increased dissociation of

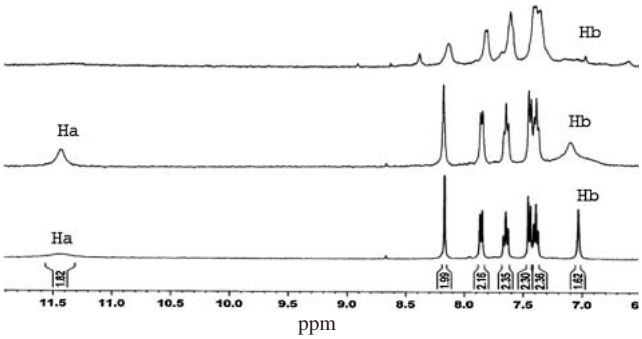

Figure 5. Showing ^{1}H NMR titration pattern (400 MHz, DMSO-d_6) (from bottom to up): Receptor **1**, **1** + 20 equivalents of $ZnCl_2$, and **1** + 100 equivalents of $ZnCl_2$.

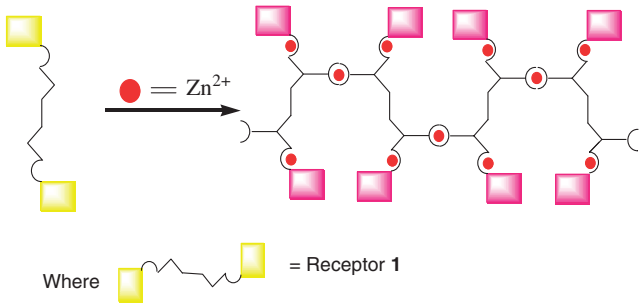

Figure 7. Proposed binding pattern of receptor **1** with Zn^{2+}.

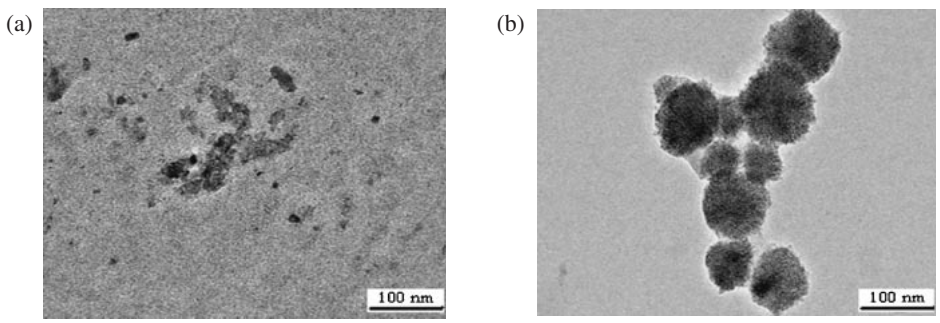

Figure 6. TEM images of receptor **1** (1.0×10^{-4} M, DMSO) before (a) and after (b) addition of 50 equivalents of $ZnCl_2$.

$ZnCl_2$ in aq. DMSO. Absolutely no UV–vis spectral changes during the addition of lower equivalents of Zn^{2+} restricted us from determining the binding affinity between receptor **1** and Zn^{2+} in terms of binding constant. At the same time our best possible efforts to develop single crystals of the resulting complex between Zn^{2+} and receptor **1** as well as its composition determination were in vain.

^{1}H NMR Studies. To further look into the nature of host–guest interactions, the ^{1}H NMR titration experiments between receptor **1** (5×10^{-3} M, DMSO-d_6) and $ZnCl_2$ (0–100 equiv) were performed. The corresponding spectral changes during the titration have been appended with Supporting Information (ESI, Figure S11) while a few partial spectra have been presented in Figure 5.

At the initial level of addition of $ZnCl_2$ to the receptor **1** the hydrazine proton i.e., H_a went on sharpening with irregular marginal up- and downfield shifting up to 30 equivalents and finally vanished at 40 equivalents. On the other hand the thiazolyl –CH proton i.e., H_b went on continuous downfield shifting and broadening to such an extent that it showed merging tendency with base line at around 40 equivalents. The initial downfield shifting of the –NH and thiazolyl –CH may be understood in terms of the coordination of Zn^{2+} with ketimine N along with carbonyl of the coumarin moiety leading to formation of six-membered chelate and responsible for the red shifting of 50 nm in the 278 nm UV–vis band of receptor **1**. The vanishing of –NH may be understood in terms of its deprotonation while excessive broadening of thiazolyl –CH is supposed to be a consequence of its involvement in intramolecular hydrogen bonding with vicinal thiazolyl N leading to formation of a five-membered ring (ESI, Figure S12) and hence able to experience the quadrupolar effect of nitrogen atom. Variation of ^{1}H NMR spectra of receptor **1** on the successive additions of Zn^{2+} also indicated its aggregation because the signals for aromatic protons of the receptor **1** in the range of 7.37–8.16 ppm were upfield shifted and reduced in height. This observation is in consonance with earlier reports for similar studies.[35]

Transmission Electron Microscopic (TEM) Studies. In order to confirm Zn^{2+} triggered aggregate formation of receptor **1** during visible sensing, the transmission electron microscopic (TEM) scannings of the 1.0×10^{-4} M DMSO solution of receptor **1** as well as of the same solution having 50 equivalents of $ZnCl_2$ were carried out. The corresponding TEM images are shown in Figures 6a and 6b. As it can be seen in Figure 6a, the particle sizes are too small while Figure 6b shows comparatively very large particle size which may be attributed to aggregate formation of receptor **1**. Hence, this study strengthened our speculation regarding aggregate formation of receptor **1** in presence of Zn^{2+} on the basis of above UV–vis and ^{1}H NMR spectral titrations.

Hence, on the basis of UV–visible, ^{1}H NMR spectral studies along with TEM scanning, the most probable pathway for the sensing of Zn^{2+} through receptor **1** may be given in Figure 7.

Conclusion

Thus we have synthesized, characterized, and demonstrated a coumarin-based ICT probe which acted as a visible receptor for Zn^{2+} as its chloride salt in aqueous DMSO (10:90 v/v) as well as in dry DMSO. The synthetic protocol for the receptor **1** is simple and cost effective also as it involves pretty cheap starting materials. The bathochromic shifting of 120 nm in one

of its ICT band (375 nm) of the receptor **1** on its binding with Zn^{2+} is a unique and rare report of its kind. Moreover the naked eye detection of Zn^{2+} at sub-millimolar level by the receptor **1** is quite up to the mark in the wake of concentration range of the same in living cells.

KKU gratefully acknowledges the financial help from UGC [F. No. 33-274/2007(SR)] New Delhi while RKM acknowledges gratefully the financial support from CSIR, New Delhi for SRF(NET). Authors are thankful to the coordinator SAP, Department of Chemistry, BHU for enabling Gaussian 03 package. We are also thankful to Prof. O. N. Srivastava, Department of Physics, BHU, Varanasi for making available TEM facility.

Supporting Information

^{1}H, ^{13}C NMR, LC-MS, and HRMS spectra for the receptor **1**, UV–vis spectra for different metal ions and for aqueous solution along with ^{1}H NMR titration spectra have been provided. This material is available free of charge on the web at http://www.csj.jp/journals/bcsj/.

References

1 A. P. de Silva, H. Q. N. Gunaratne, T. Gunnlaugsson, A. J. M. Huxley, C. P. McCoy, J. T. Rademacher, T. E. Rice, *Chem. Rev.* **1997**, *97*, 1515.

2 P. A. Gale, *Coord. Chem. Rev.* **2000**, *199*, 181.

3 F. P. Schmidtchen, M. Berger, *Chem. Rev.* **1997**, *97*, 1609.

4 P. D. Beer, P. A. Gale, *Angew. Chem., Int. Ed.* **2001**, *40*, 486.

5 F. J. J. R. da Silva, R. J. P. Williams, *The Biological Chemistry of the Elements*, 2nd ed., Oxford University Press, New York, **2001**.

6 E. Kimura, *Acc. Chem. Res.* **2001**, *34*, 171.

7 S. Y. Assaf, S.-H. Chung, *Nature* **1984**, *308*, 734.

8 J. M. Berg, Y. Shi, *Science* **1996**, *271*, 1081.

9 E. M. Nolan, S. J. Lippard, *Acc. Chem. Res.* **2009**, *42*, 193.

10 E. F. Rostan, H. V. DeBuys, D. L. Madey, S. R. Pinnell, *Int. J. Dermatol.* **2002**, *41*, 606.

11 Z. Szitányi, C. Nemes, N. Rozlosnik, *Cent. Eur. J. Occup. Environ. Med.* **1998**, *4*, 51.

12 M. J. Salgueiro, M. B. Zubillaga, A. E. Lysionek, R. A. Caro, R. Weill, J. R. Boccio, *Nutrition* **2002**, *18*, 510.

13 Z.-P. Yu, G.-W. Le, Y.-H. Shi, *Clin. Exp. Pharmacol. Physiol.* **2005**, *32*, 273.

14 M. Ferenčík, L. Ebringer, *Folia Microbiol.* **2003**, *48*, 417.

15 C. J. Frederickson, *Int. Rev. Neurobiol.* **1989**, *31*, 145.

16 K. K. Upadhyay, A. Kumar, R. K. Mishra, T. M. Fyles, S. Upadhyay, K. Thapliyal, *New J. Chem.* **2010**, in press. doi:10.1039/c0nj00097c

17 K. K. Upadhyay, R. K. Mishra, V. Kumar, P. K. Roy Chowdhury, *Talanta* **2010**, *82*, 312.

18 K. K. Upadhyay, A. Kumar, S. Upadhyay, R. K. Mishra, P. K. Roychoudhuary, *Chem. Lett.* **2008**, *37*, 186.

19 K. K. Upadhyay, A. Kumar, R. K. Mishra, R. Prasad, *Bull. Chem. Soc. Jpn.* **2009**, *82*, 813.

20 K. K. Upadhyay, R. K. Mishra, A. Kumar, J. Zhao, R. Prasad, *J. Mol. Struct.* **2010**, *963*, 228.

21 K. K. Upadhyay, A. Kumar, J. Zhao, R. K. Mishra, *Talanta* **2010**, *81*, 714.

22 J. Orbulescu, P. Kele, A. Kotschy, R. M. Leblanc, *J. Mater. Chem.* **2005**, *15*, 3084.

23 J. D. Winkler, C. M. Bowen, V. Michelet, *J. Am. Chem. Soc.* **1998**, *120*, 3237.

24 E. M. Nolan, J. Jaworski, M. E. Racine, M. Sheng, S. J. Lippard, *Inorg. Chem.* **2006**, *45*, 9748.

25 F. A. Khan, K. Parasuraman, K. K. Sadhu, *Chem. Commun.* **2009**, 2399.

26 C. C. Woodroofe, S. J. Lippard, *J. Am. Chem. Soc.* **2003**, *125*, 11458.

27 H. Miyaji, H.-K. Kim, E.-K. Sim, C.-K. Lee, W.-S. Cho, J. L. Sessler, C.-H. Lee, *J. Am. Chem. Soc.* **2005**, *127*, 12510.

28 K. R. Romines, J. K. Morris, W. J. Howe, P. K. Tomich, M.-M. Horng, K.-T. Chong, R. R. Hinshaw, D. J. Anderson, J. W. Strohbach, S. R. Turner, S. A. Mizsak, *J. Med. Chem.* **1996**, *39*, 4125.

29 I. Raad, R. Terreux, P. Richomme, E.-L. Matera, C. Dumontet, J. Raynaud, D. Guilet, *Bioorg. Med. Chem.* **2006**, *14*, 6979.

30 F. Knoevenagel, *Ber. Dtsch. Chem. Ges.* **1898**, *31*, 730.

31 R. S. Lokhande, S. Nirupa, A. B. Chaudhary, *Asian J. Chem.* **2002**, *14*, 149.

32 M. J. Frisch, G. W. Trucks, H. B. Schlegel, G. E. Scuseria, M. A. Robb, J. R. Cheeseman, J. A. Montgomery, Jr., T. Vreven, K. N. Kudin, J. C. Burant, J. M. Millam, S. S. Iyengar, J. Tomasi, V. Barone, B. Mennucci, M. Cossi, G. Scalmani, N. Rega, G. A. Petersson, H. Nakatsuji, M. Hada, M. Ehara, K. Toyota, R. Fukuda, J. Hasegawa, M. Ishida, T. Nakajima, Y. Honda, O. Kitao, H. Nakai, M. Klene, X. Li, J. E. Knox, H. P. Hratchian, J. B. Cross, V. Bakken, C. Adamo, J. Jaramillo, R. Gomperts, R. E. Stratmann, O. Yazyev, A. J. Austin, R. Cammi, C. Pomelli, J. W. Ochterski, P. Y. Ayala, K. Morokuma, G. A. Voth, P. Salvador, J. J. Dannenberg, V. G. Zakrzewski, S. Dapprich, A. D. Daniels, M. C. Strain, O. Farkas, D. K. Malick, A. D. Rabuck, K. Raghavachari, J. B. Foresman, J. V. Ortiz, Q. Cui, A. G. Baboul, S. Clifford, J. Cioslowski, B. B. Stefanov, G. Liu, A. Liashenko, P. Piskorz, I. Komaromi, R. L. Martin, D. J. Fox, T. Keith, M. A. Al-Laham, C. Y. Peng, A. Nanayakkara, M. Challacombe, P. M. W. Gill, B. Johnson, W. Chen, M. W. Wong, C. Gonzalez, J. A. Pople, *Gaussian 03, Revision B.05*, Gaussian, Inc., Wallingford CT, **2004**.

33 R. H. Abu-Eittah, B. A. H. El-Tawil, *Can. J. Chem.* **1985**, *63*, 1173.

34 Y. Fu, H. Li, W. Hu, *Eur. J. Org. Chem.* **2007**, 2459.

35 L. Liu, G. Zhang, J. Xiang, D. Zhang, D. Zhu, *Org. Lett.* **2008**, *10*, 4581.